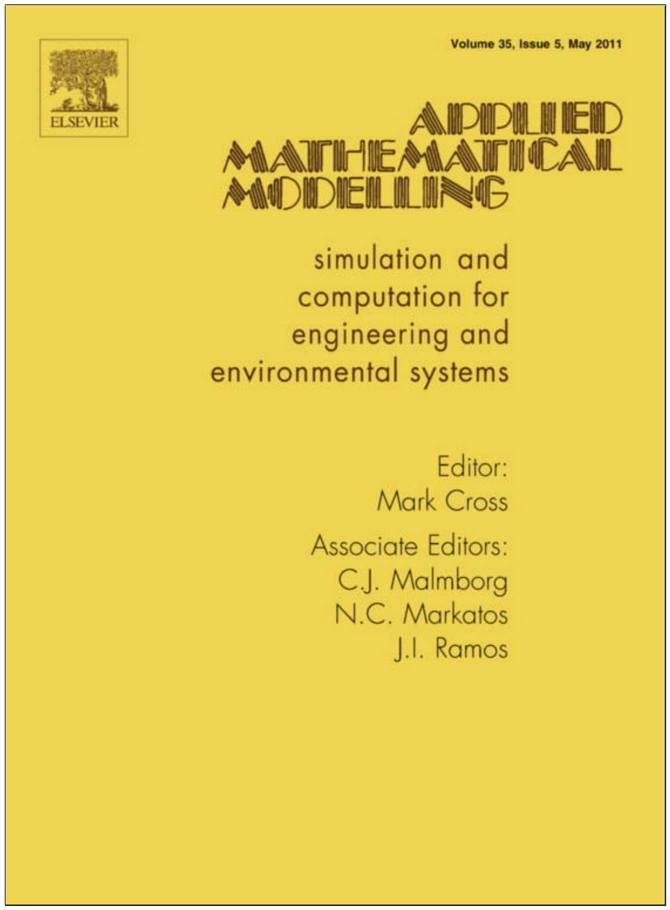
Volume 35, Issue 5, May 2011
ELSEVIER
APPLIED MATHEMATICAL MODELLING
simulation and computation for engineering and environmental systems
Editor:
Mark Cross
Associate Editors:
C.J. Malmborg
N.C. Markatos
J.I. Ramos

Applied Mathematical Modelling 35 (2011) 2324–2335

Contents lists available at ScienceDirect

Applied Mathematical Modelling

journal homepage: www.elsevier.com/locate/apm

Nonlinear mathematical modeling of butterfly valves driven by solenoid actuators

Peiman Naseradinmousavi *, C. Nataraj

Villanova University, Mechanical Engineering Department, 800 Lancaster Avenue, Villanova, PA 19085, United States

A R T I C L E   I N F O

Article history:
Received 11 January 2010
Received in revised form 5 November 2010
Accepted 15 November 2010
Available online 25 November 2010

Keywords:
Dynamic systems modeling
Nonlinear modeling
Solenoid actuator
Butterfly valve
Nonlinear dynamics

A B S T R A C T

This paper describes high fidelity modeling and analysis of the opening and closing processes of butterfly valves driven by solenoid actuators using multiphysics models. The equations are derived and solved numerically. The variable of primary interest is the butterfly valve rotation angle. The coupled model for electromagnetics, fluid dynamics and mechanical dynamics are derived by making some simplifying assumptions. It is shown that the behavior of hydrodynamic torque plays an important role in the closing and opening processes. A discussion is presented with an explanation of the results and a comparison has been made for both the processes.

Published by Elsevier Inc.

1. Introduction

In order to support the next generation Naval machinery automation requirements, predictive and adaptive shipboard machinery systems have been proposed [1]. Their objective has been to enable real time predictive capability to help achieve a much higher degree of autonomy than has been achieved so far. This paper analyzes a critical part of the automation system, namely, actuator-valve systems that form an important part of what are termed “smart valve” systems. It is expected that the present research will add to the suite of analytical and numerical tools in addition to providing insight for dynamic performance prediction and control systems design.

Typical automation systems used in the US Navy consist of actuators, sensors, controllers, valves, piping, electrical cabling and communication wiring. Many types of valves are in use [2,3]. Gate valves, where the disk is in the shape of a “gate” or wedge are often used as isolating valves for pieces of equipment or key components, such as control valves, for service during maintenance and repair. Globe valves consist of a round disk or plug-type disk seated against a round port and are sometimes called balancing valves. Check valves are used to prevent, or check, reverse flow. Butterfly valves have a thin rotating disk and may be used for throttling purposes in addition to on/off control. Water control valves can again be classified as two-way and three-way mixing or diverting valves.

All of these valves are nonlinear; but it is common engineering practice to linearize the characteristic curves about operating points, and to ignore the nonlinearities for all aspects of modeling, design and control. For most control valves, a plot of the flow versus valve position is nonlinear. Most control system designs take the slope (valve gain) as the basis for a linearized model. If we were to plot a process variable versus this flow, such as temperature or composition, it would also be nonlinear. Here the slope would be the process gain. These are called operating point nonlinearities. If the process variable stays close to its set point, the slope does not change much. Thus, for a constant set point, minimal dead time, and good

* Corresponding author. Tel.: +1 4846204648.
E-mail address: pnaser01@villanova.edu (P. Naseradinmousavi).

0307-904X/$ - see front matter Published by Elsevier Inc.
doi:10.1016/j.apm.2010.11.036

tuning, the process nonlinearity is not much of an issue. On the other hand, the control valve may have to move significantly to achieve tight control. The control loop is then more likely to be affected by the nonlinearity of the control valve. Generally the slope of the installed characteristic gets flat at low and high positions.

This paper will focus in particular on solenoid actuated butterfly valves and follows up the previous work done by the authors [4]. There have been numerous papers focusing on the valve analysis driven by pneumatic actuators coupled by a rack and pinion mechanism because of its high precision of operation and offering rapid responses which have been employed by several manufacturers and companies. The industries offer a wide range of valves including butterfly types coupled by a spring to save the usage of energy and driven by pneumatic-based actuators.

There is a very limited amount of research on accurate dynamic modeling of valves driven by solenoid actuators. This paper exploits the ideas of using a spring and damper to yield smoother responses for the system coupled by a rack and pinon mechanism utilizing a solenoid actuator, the modulating type as shown in Fig. 1a, instead of the pneumatic types. The geometrical parameters of the solenoid are the same as shown in Fig. 2 [5] for the calculation of values of the path's reluctance. In a solenoid actuator, the key aim is to close and open quickly which is a motivation to consider its nonlinear behavior for the valve opening and closing processes. It is a strongly nonlinear device and needs to be modeled as such.

2. Mathematical modeling

The system consists of a solenoid actuator energized by an electric voltage (DC or AC) which moves a plunger. The plunger is connected to a butterfly valve through a rack and pinion arrangement. The magnetic flux generates the needed electromagnetic force to move the plunger and subsequently results in the rotation of the butterfly valve by the coupled rack and pinion mechanism. An ideal pressure angle is assumed for the rack and pinion mechanism with an assumption of no backlash of the gears. The valve controls the flow in a pipe and is hence subject to hydrodynamic forces. The investigations of the opening and closing processes of the valve indicate differences regarding the behavior of hydrodynamic torque. The hydrodynamic torque results in a nonlinear resistance and an aiding torque for the opening and closing processes, respectively.

2.1. Electromagnetics

There has been some recent work on modeling and analysis of solenoid actuators [5–11]. The work by Zavarehi et al. [7] and Rahman et al. [8] is similar to our model of the solenoid actuators. The assumptions include small air gaps between the plunger and yoke, and negligible fringing, leakage, and eddy currents. Also, ignoring saturation and magnetic field nonlinearity leads to the following.

$$B = \mu H, \tag{1}$$

where, B is the magnetic flux density, H is the magnetic field strength, and μ is the magnetic permeability.

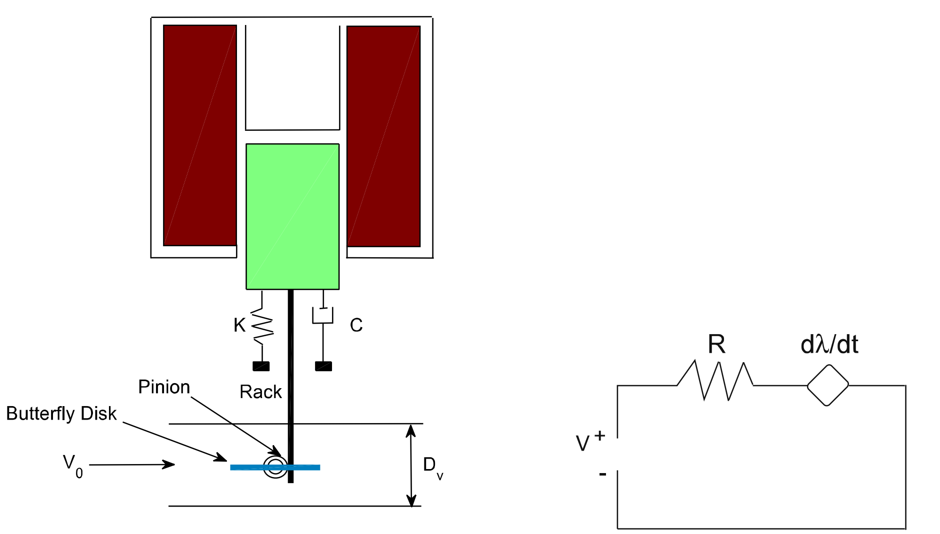

(a) Schematic model (b) Solenoid actuator electric circuit

Fig. 1. Schematic models of the system and the solenoid electric circuit.

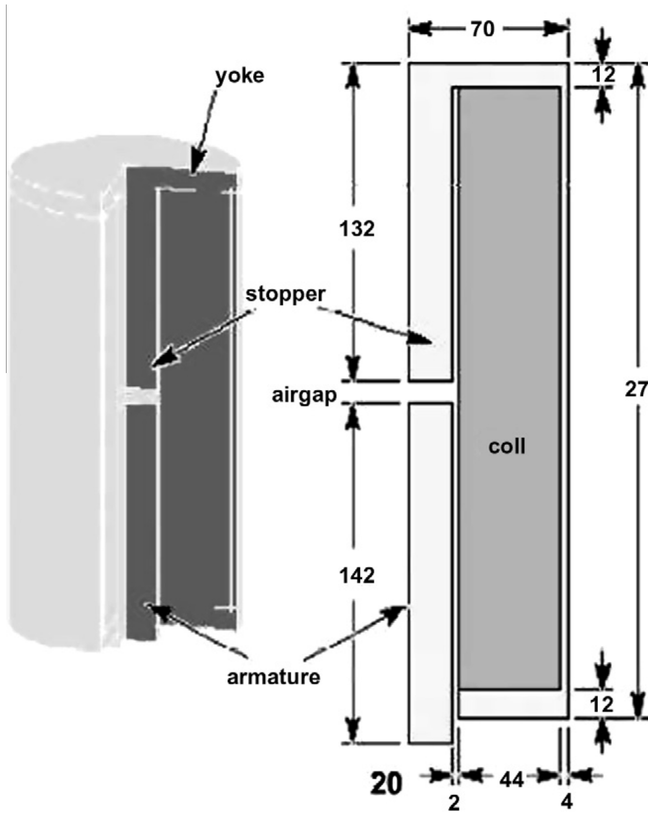

Fig. 2. Solenoid actuator configuration in millimeter [5].

Using Ampere's circuital law for the magnetic motive force, the magnetic field intensity is proportional to the current, i, and the number of coils, N. Applying it to the magnetic circuit,

$$\oint H d\ell = Ni, \tag{2}$$

where, ℓ is the length of the closed magnetic path (m). λ, the flux linkage (Wb) and ϕ, the magnetic flux are related as follows:

$$\lambda = N\phi. \tag{3}$$

Also, simplifying Eq. (2) and combining with Eq. (3) with respect to the stated $B - H$ relationship, one has,

$$R_i = \frac{l_i}{\mu_i S_i}, \tag{4}$$

$$\phi = \frac{Ni}{\sum_{i=1}^{n} R_i}, \tag{5}$$

where, S_i is the projected cross-sectional area of the media normal to the magnetic flux, and R_i is reluctance of the media. Note that the magnetic flux has an inverse relation with the reluctance. Using the principle of virtual work, the electromagnetic force can be computed by the following relationship.

$$F_{\text{mag}} = \frac{\partial W_{\text{co-energy}}}{\partial x}. \tag{6}$$

By definition,

$$F_{\text{mag}} = \frac{\partial}{\partial x} \int_0^i \lambda(x, i) di. \tag{7}$$

The reluctance of Eq. (4) can be shown to be represented by the following relation for the closing process.

$$\sum_{i=1}^{n} R_i = C_1 + C_2 x. \tag{8}$$

For all the above relations, x indicates the displacement of solenoid plunger (which is the air gap). Combining Eqs. (3), (5) and (8), the total generated electromagnetic force for upward motion of the plunger can be calculated as follows.

$$F_{\text{mag}} = \frac{C_2 N^2 i^2}{2(C_1 + C_2(g_{max} - x))^2}, \tag{9}$$

where g_{mag} shows the maximum stroke of plunger.

Eq. (9) demonstrates strong nonlinearity among the generated electromagnetic force, current, and plunger displacement. Note that all the stated equations are just valid for the closing process of the valve which is accomplished by the upward vertical motion of the plunger. The solenoid actuator can be modeled as an electronic circuit as shown in Fig. 1b.

$$V = Ri + \frac{d\lambda}{dt}. \tag{10}$$

Combining Eqs. (3), (4), (5), and (10), a state equation can be written for the current.

$$\frac{di}{dt} = \frac{(V - Ri)(C_1 + C_2(g_{max} - x))}{N^2} - \frac{C_2 i\dot{x}}{(C_1 + C_2(g_{max} - x))}. \tag{11}$$

2.2. Fluid mechanics

As shown in Figs. 1a and 3, the butterfly valve rotation angle is affected by the hydrodynamic torque exerted by the fluid flow in the pipes, which has been subject to some experimental and theoretical investigations. Hydrodynamic torque acting on a butterfly valve has been researched by [12–15]. As shown in Fig. 3, the ratio of the jet (V_J, between the wall boundary and the free-flow streamline) and inlet velocities of channel (V_0) is written as follows [12]:

$$\frac{V_J}{V_0} = \frac{2}{(C_{c1} + C_{c2})(1 - \sin(\alpha))}, \tag{12}$$

where, C_{c1} and C_{c2} are upper and lower contraction coefficients. Shown in Fig. 4a is the sum of C_{c1} and C_{c2} versus the valve rotation angle for both the opening and closing processes of the valve.

The hydrodynamic torque (T_h) is given by the following equation.

$$T_h = \frac{8\rho T_c D_v^3 V_0^2}{3\pi}\left(\frac{V_J}{V_0}\right)^2. \tag{13}$$

Combining Eqs. (12) and (13), the hydrodynamic torque is written as follows.

$$T_h = \frac{32\rho T_c D_v^3 V_0^2}{3\pi[(C_{c1} + C_{c2})(1 - \sin(\alpha))]^2}, \tag{14}$$

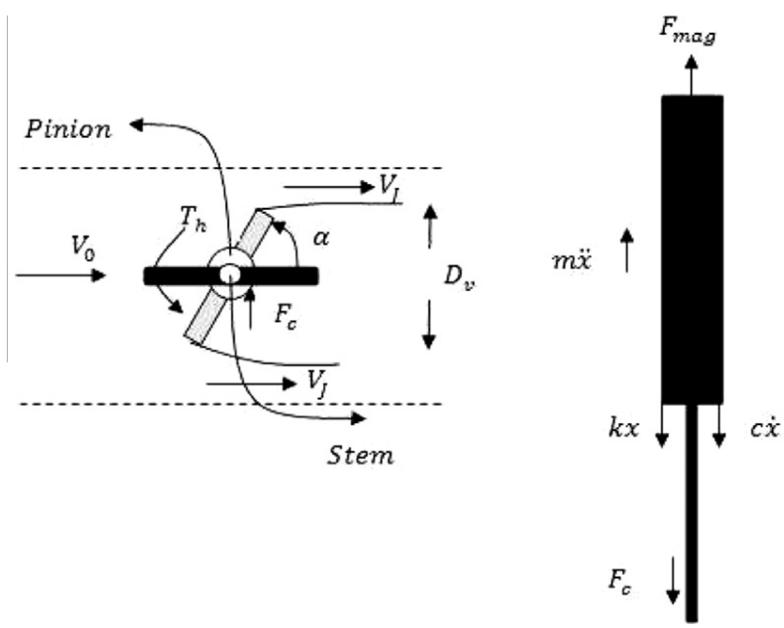

Fig. 3. The free body diagrams of both the butterfly valve and solenoid actuator.

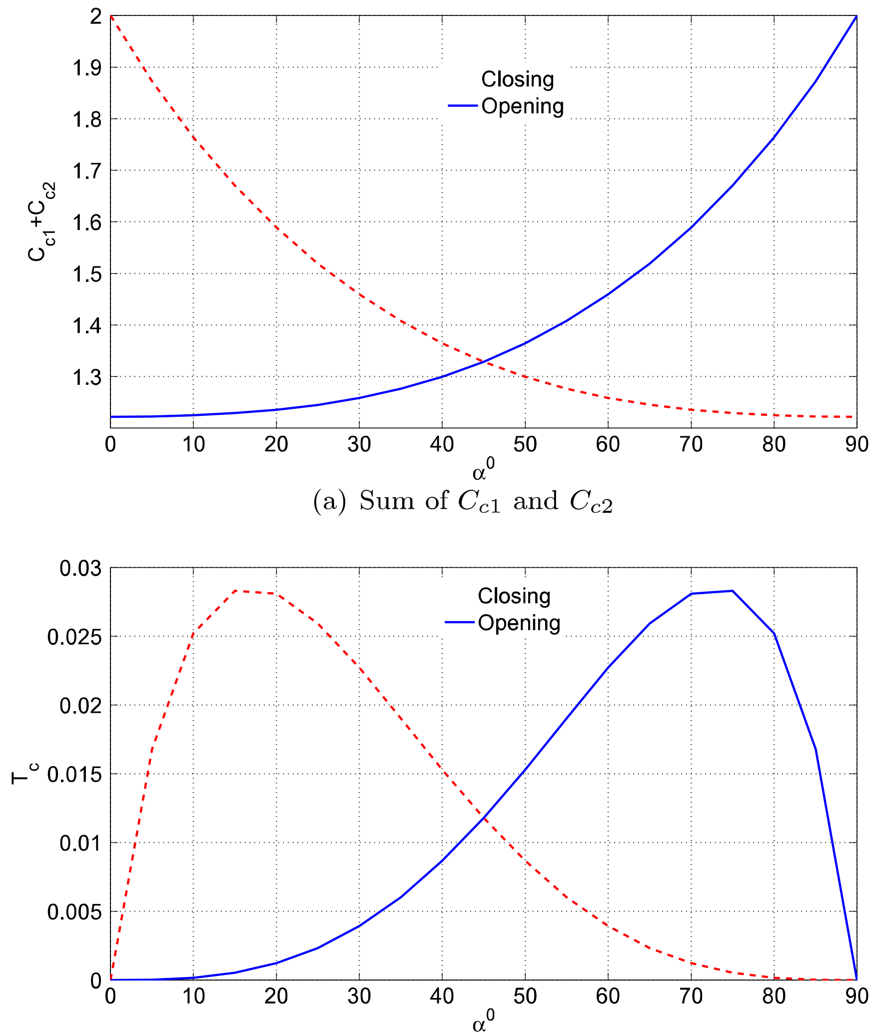

(a) Sum of C_{c1} and C_{c2}

(b) Hydrodynamic coefficient

Fig. 4. Sum of C_{c1} and C_{c2} and hydrodynamic coefficient for both of the opening and closing processes.

where, ρ is the fluid density; T_c is the torque coefficient; D_v is the pipe diameter, and α presents the valve rotation angle. The torque coefficient value can be calculated by a table look up process versus the valve rotation angle. With all parameters being constant, the variation of the torque coefficient with the rotation angle is illustrated in Fig. 4b for both the opening and closing processes of the valve. It is clear that the relationship is strongly nonlinear. Note that these relations were obtained from a Computational Flow Dynamic calculation and do not have explicit analytical expressions.

In addition to the hydrodynamic torque affecting the rotation angle of the valve, the bearing torque is another prominent effect which must be investigated. We present the methods of calculations of both the compressible and incompressible flows. The experimental relation stating the magnitude of bearing torque, for a compressible flow, was derived by [16].

$$T_{b,comp} = \frac{\pi}{8}\mu D_s C_R D_v^2 \Delta P. \tag{15}$$

In extracting Eq. (15), ΔP is calculated as follows.

$$\Delta P = \frac{1}{2}\rho K V_0^2, \tag{16}$$

where,

$$K = \left(\frac{V_J}{V_0} - 1\right)^2. \tag{17}$$

Since C_R is dependent on the disk geometry, disk position, and valve pressure ratio (VPR), the exact value is likely unknown. However, C_R is dependent on both the lift and drag force coefficients and can be expressed by

$$C_R = \sqrt{C_L^2 + C_D^2}. \tag{18}$$

Modeling C_L and C_D using powers of the sine and cosine functions based on the behavior of the individual coefficients for a fluid operating at conditions included in [16], and approximating their behavior at disk positions of 0 deg and 90 deg yields the following approximations.

$$C_L = 1.1\sqrt[4]{\sin\left(\left(\frac{\alpha}{90}\right)^3 180\right)}, \tag{19}$$

$$C_D = \sqrt[3]{\cos(\alpha)}. \tag{20}$$

Eqs. (19) and (20) are strictly empirical and were developed from a curve fit to the measured results. For incompressible flow [17], the bearing torque is as follows.

$$T_{b,water} = \frac{\pi}{8}\mu D_s D_v^2 \Delta P. \tag{21}$$

Clearly, the bearing torque would always act in a direction opposite to that of the valve rotation.

In addition to the above, we will need to include a seating torque whose behavior is similar to that of the bearing torque. The following equation describes a relation of the seating torque and the pipe diameter [17].

$$T_s = C_s D_v^2, \tag{22}$$

where, C_s is the coefficient of the seating area.

Adding the torques calculated by Eqs. (14), (15), and (22), the total toque on the valve is obtained. Clearly, it has a highly nonlinear relationship with the valve rotation angle.

2.3. Dynamics

As stated earlier, the dynamical equations must be modified with respect to the opening and closing processes of the valve. As shown in Fig. 3, for the closing process, the dynamical equations of the plunger and butterfly valve can be written as the following.

$$m\ddot{x} + c\dot{x} + kx = F_{\text{mag}} - F_c, \tag{23}$$

$$J\ddot{\alpha} + b\dot{\alpha} = rF_c + T_h - T_b - T_s, \tag{24}$$

where, m is the mass of the solenoid plunger; T_{b} is the bearing torque; T_{h} shows the hydrodynamic torque; k is spring stiffness; c indicates damping coefficient. For the opening process, the EOM can be written as follows.

$$J\ddot{\alpha} + b\dot{\alpha} = rF_c - T_h - T_b - T_s. \tag{25}$$

2.4. Numerical results

A Simulink model was developed based on the equations presented for modeling of the butterfly valve driven by the solenoid actuator for both the opening and closing processes of the valve. The parameters used in the simulation are given in Table 1. We examine both the regular (springless) and modulating (with spring) actuators. For both the processes, Figs. 5–7 show the applied currents, vertical displacements and velocities of plunger, and finally valve rotation angles for the various magnitudes of the inlet velocities. Fig. 5a shows the applied current of the solenoid (using regular type) for both the compressible and incompressible flows where important differences can be noted. Considerable fluctuations can be observed while using the regular actuator without a spring and a damper. A good solution can be found in the modulating actuator

Table 1
Model parameters.

Parameters	Values
Plunger mass (m)	0.1 kg
Moment inertia of the valve disk (J)	0.104×10^{-4}
Pipe diameter (D_v)	0.2032 m
Stem diameter (D_s)	0.0254 m
Friction coefficient of bearing area (μ)	0.2
Coefficient of seating area (C_s)	0.2
C_1	1.5683×10^6
C_2	6.3207×10^8
Fluid density (ρ)	1000 kg/m^3
Relative permeability (μ_r)	630 (NA^{-2})
Radius of pinion (r)	0.05 m

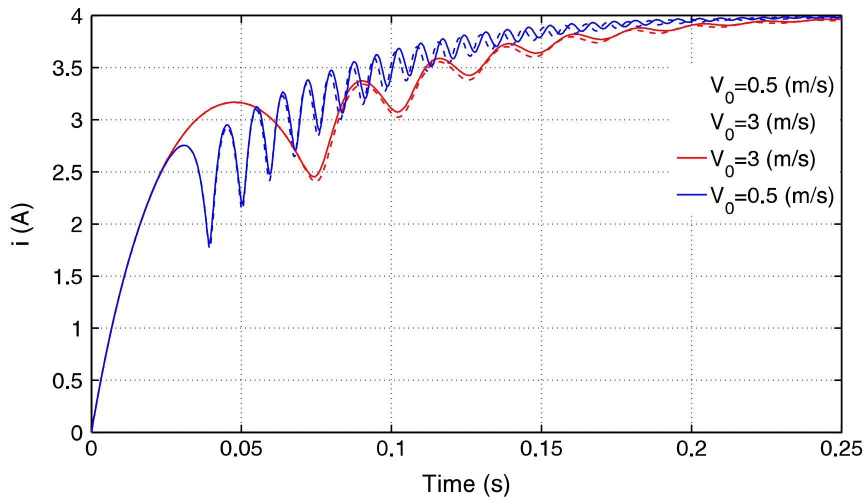

(a) Closing process; Solid lines; Water, Dashed lines; Air, $N = 3300$, $i = 4A$, $k = 0$, $c = 5(Ns)/m$

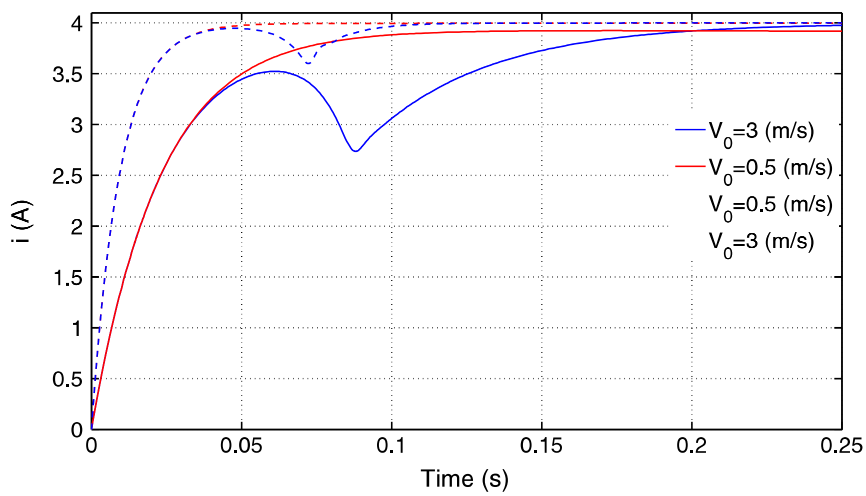

(b) Closing process; Solid lines; Water, Dashed lines; Air, $N = 3300$, $i = 4A$, $k = 400$, $c = 100(Ns)/m$

Fig. 5. Applied currents vs. time for both the compressible and incompressible flows.

which utilizes a spring and a damper for yielding smoother responses as shown in Fig. 5b. Obviously, a compromise must be made between the response time of the system and its oscillatory behavior. The stated rules are also valid for the opening process of the valve while the applied currents present considerable differences for both the compressible and incompressible flows.

Our principal interest here is the investigation of the valve behavior for incompressible flow, in particular, water. Shown in Fig. 6 are several aspects of the different behaviors of hydrodynamic torque for both the closing and opening processes. For the closing process, both the plunger vertical motion and disk rotation take shorter times to reach their steady state values with increasing values of the inlet velocities of the flow. The variables (x and α) show different behaviors for the opening process while slower responses can be observed which is probably due to resistance behavior of the hydrodynamic torque.

Increasing values of the inlet velocities result in considerably smaller values of both the plunger displacements and subsequently the valve rotation angles for the opening process than the values of the closing process. This point can be used for the optimization of energy since the closing process seems to be more effective yielding higher values of the valve rotation angles for the same applied currents than those of the opening process. The plunger velocity has behavior similar to that of the plunger displacements regarding the opening and closing processes as can be seen in Fig. 7. The figure indicates much higher values of the plunger velocities for the closing process than for the opening process.

As can be seen in Fig. 8a and b, higher steady state values are seen for the total acting torques for the opening process due to their additive terms than that of the closing process. A variation in the number of coils can be examined to evaluate the performance and response times of the system for both the processes. Fig. 9a and b presents the effects of different values of N for the plunger displacements; the valve rotation angle follows the same behavior. Increasing values of N result in slower

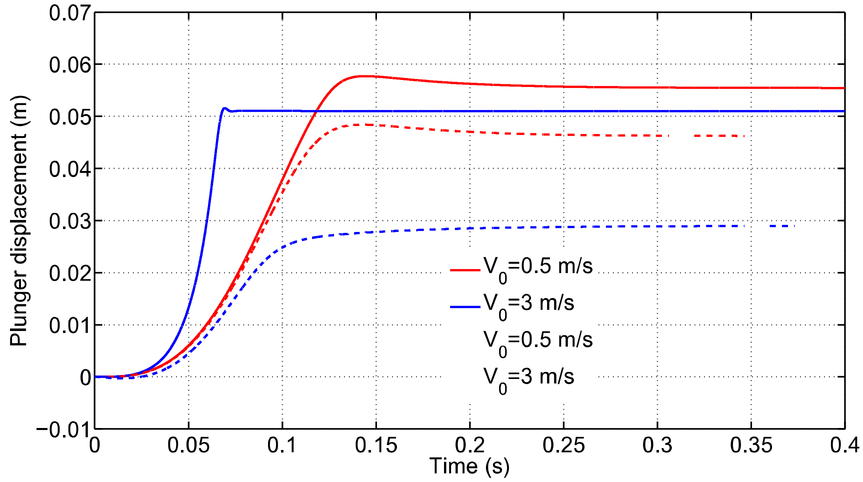

(a) Solid lines; closing, Dashed lines; opening, $N = 3300$, $i = 4A$, $k = 400(N/m)$, $c = 100(Ns)/m$

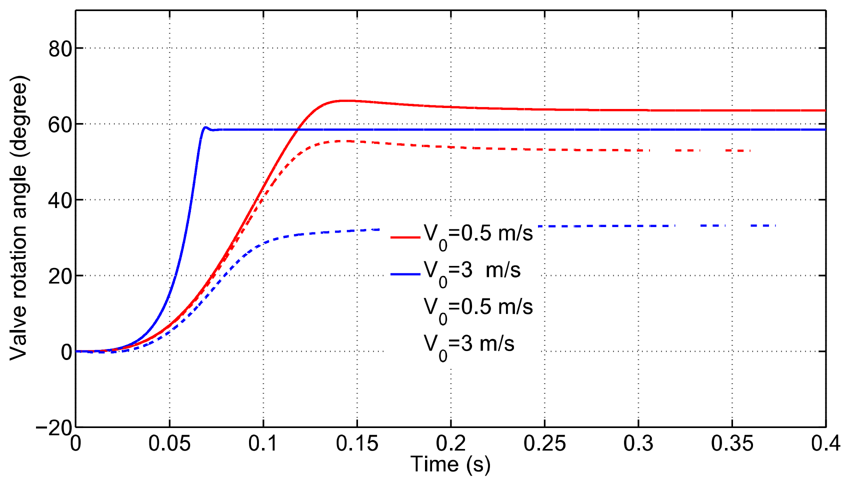

(b) Solid lines; closing, Dashed lines; opening, $N = 3300$, $i = 4A$, $k = 400(N/m)$, $c = 100(Ns)/m$

Fig. 6. Plunger displacements and valve rotation angles.

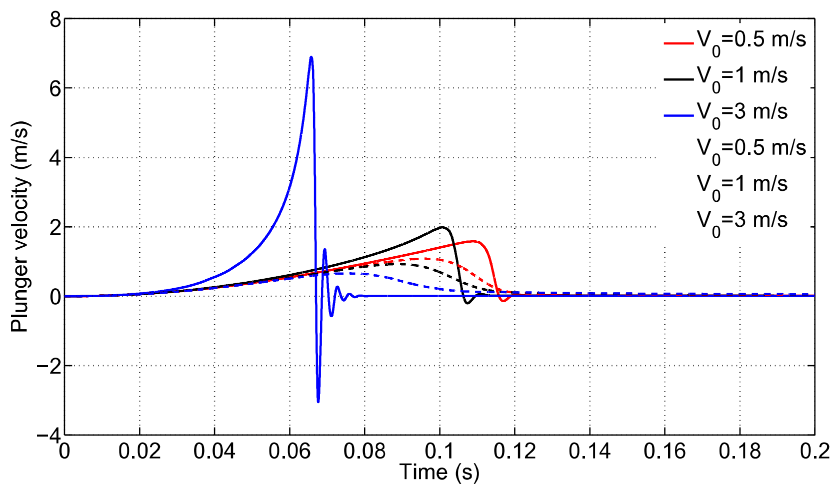

Fig. 7. Plunger velocities vs. time for; Solid lines; closing, Dashed lines; opening, $N = 3300$, $i = 4A$, $k = 400$ N/m, $c = 100$ N/(m/s).

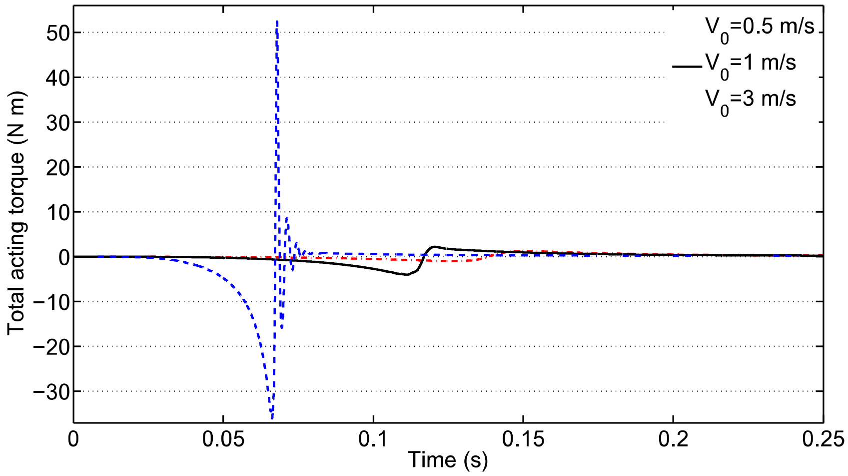

(a) Closing process, $N = 3300$, $i = 4A$, $k = 400(N/m)$, $c = 100(Ns)/m$, $T_b + T_s - Th$

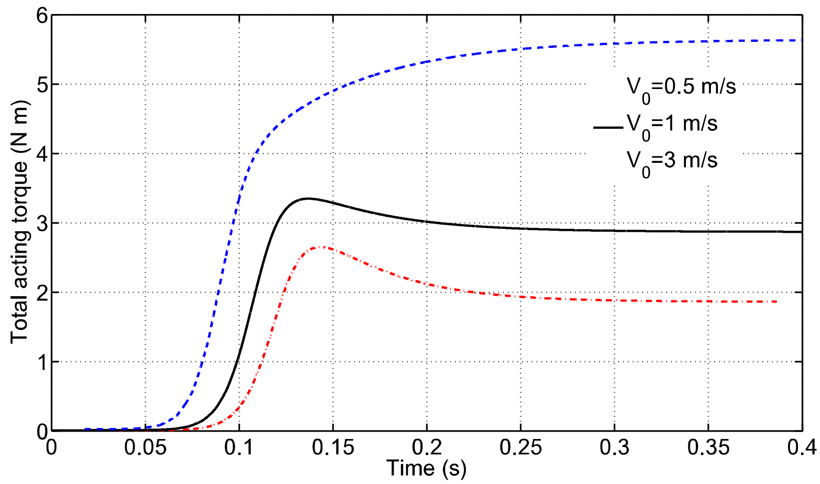

(b) Opening process, $N = 3300$, $i = 4A$, $k = 400(N/m)$, $c = 100(Ns)/m$, $T_b + T_s + Th$

Fig. 8. Total acting torques.

response times of the system while it yields higher values of the valve rotation angles and plunger displacements for both the opening and closing processes (as expected). The rate of current, on the other hand, has an inverse relationship with the number of coils yielding slower response times to reach their steady state values as can be seen in Fig. 10.

Consequently, the electromagnetic force follows the same behavior in that it has a direct relationship with the applied current yielding slower response times and higher values of the both plunger displacements and the valve rotations. A suitable controller can be designed to drive the valve to the desired angles. An adaptive controller has been developed by the authors and is reported elsewhere [18]. As might be expected, higher values of control currents show higher values of the valve rotation angles.

It should be noted that increasing the number of coils and/or the current could invalidate the linear field assumptions made in deriving the model and invalidate the results.

Shown in Fig. 11 is the complete process of the valve opening and closing with the selected sequence of closing/opening regarding the used modulating actuator when the current presents 4*A*. Obviously, the plunger exhibits the same behavior as the valve.

3. Discussion

Regarding Figs. 6 and 8, one can observe smoother profiles of the hydrodynamic torques affecting the butterfly valve rotation angles due to the modulating actuator with a spring. Obviously, increases of the inlet velocities yield shorter response times of the valve closing process while it generates slower response times with increasing values of the number of coils as

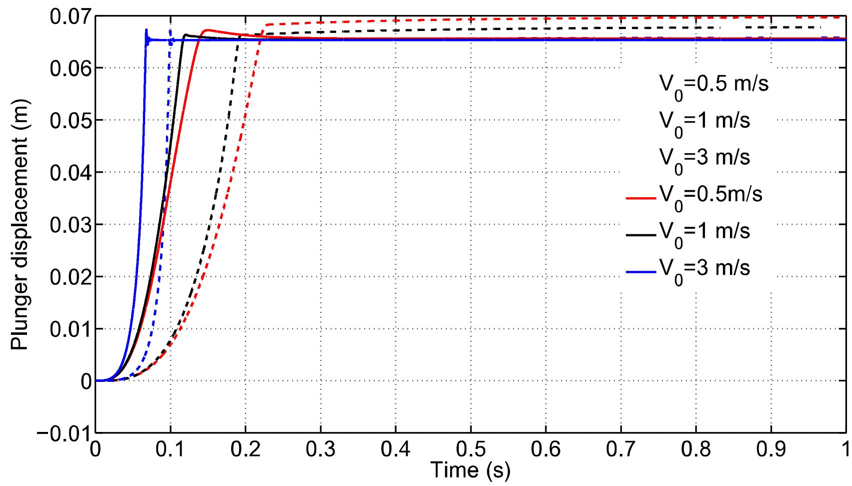

(a) Closing process, Solid lines; $N = 3300$, Dashed lines; $N = 8800$, $i = 4A$, $k = 400(N/m)$, $c = 100(Ns)/m$

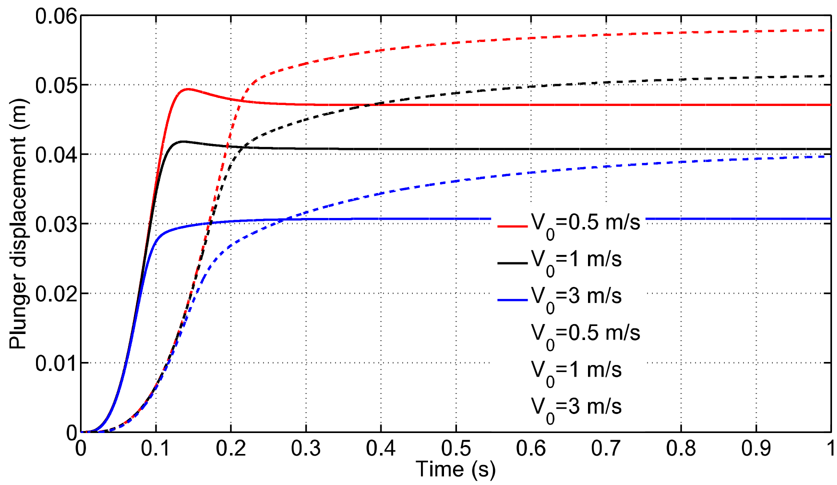

(b) Opening process

Fig. 9. Plunger displacements for two values of *N*.

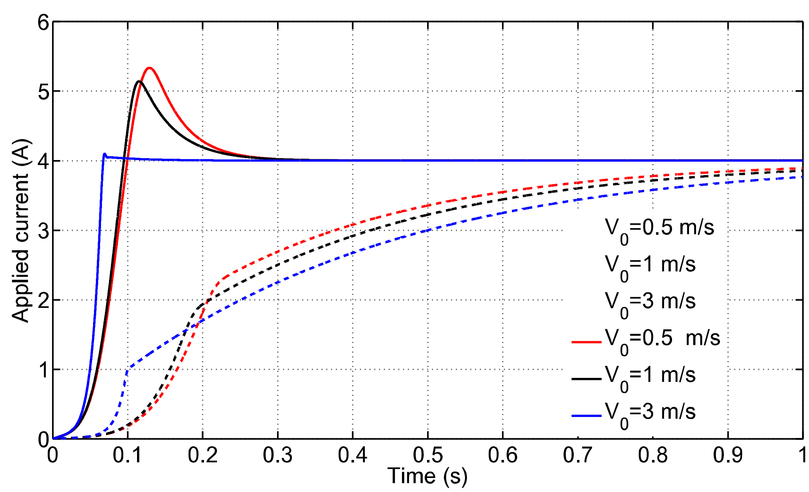

Fig. 10. Applied currents vs. time for; Solid lines; $N = 3300$, Dashed lines; $N = 8800$, $i = 4A$, $k = 400$ N/m, $c = 100$ N/(m/s).

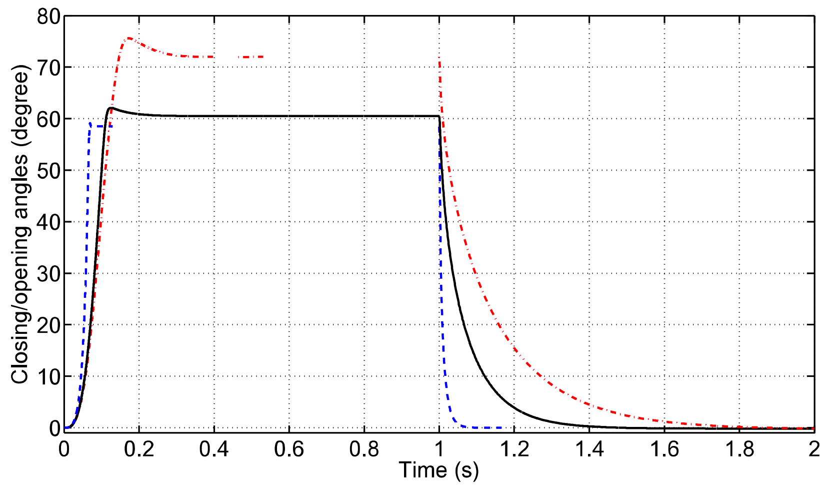

Fig. 11. Complete closing and opening processes of the valve; Dotted line; $V_0 = 0.5$ m/s, Solid line; $V_0 = 1$ m/s, Dashed line; $V_0 = 3$ m/s, $k = 400$ N/m, $c = 100$ N/(m/s).

shown in Figs. 6 and 9. Also, higher values of both the opening and closing angles can be observed by increasing values of the number of coils. Note that one is able to distinguish between decreasing values of the valve opening angles and slower response times of the opening process with increasing values of the inlet velocities in comparison with the closing process. Increasing values of the control currents lead to the same behavior for both the closing and opening processes.

The analysis provides a clear picture of the underlying physical and mathematical process. The analytical model also provides a basis for design improvements, and a convenient and manageable mathematical model for parametric studies. In addition, any design optimization is only possible with a simpler model such as the analytical model. Finally, the controller design would simply not be possible without an analytical model.

4. Conclusions

This paper developed accurate analytical models for butterfly valves operated by solenoid actuators. Analytical equations are derived and solved. The generated electromagnetic force of the solenoid actuator is modeled using magnetic circuit equations. A rack and pinion mechanism has been used due to its high precision of operation and rapid responses. The model has been studied for both the compressible (air) and incompressible (water) flows regarding the differences of the bearing torque's term for both the opening and closing processes.

The effects of the system parameters on the dynamic response have been investigated. The sequence of operation has been selected while the closing/opening process using a modulating solenoid yields optimum responses of the system. Also, several design parameters are identified. All indications from the simulations are that there are several important nonlinear dynamic phenomena present especially at higher speeds. Current work is focusing on a nonlinear dynamic analysis with a nondimensional model as well as an adaptive controller.

Acknowledgements

This work was supported by Office of Naval Research Grant. The authors are grateful to ONR, and Mr. Anthony Seman III in particular, for the financial support that made this research possible. Thanks are also due to Dr. Stephen Mastro of Naval Surface Warfare Center (Philadelphia) for valuable help and guidance.

References

[1] A. Seman, Adaptive automation for machinery control, ONR Presentation (2007).
[2] Johnson Control, Inc., Valve and Actuator Manual 977, 1994, Engineering Data Book Vb1, Code No LIT-347Vb.
[3] Tyco Flow Controls, Navy and commercial marine products, Prod. Brochure. (2007).
[4] C. Nataraj, P.N. Mousavi, Nonlinear Analysis of Solenoid Actuators and Butterfly Valve Systems, 14th International Ship Control Systems Symposium, Ottawa, Canada, 2009, pp. 1–8.
[5] J.R. Brauer, Magnetic diffusion times for infusion and effusion in nonlinear steel slabs and cylinders, IEEE Trans. Magnet. 43 (7) (2007) 3181–3188.
[6] J.R. Brauer, Magnetic Actuators and Sensors, Wiley IEEE Press, New Jersey, 2006.
[7] M.K. Zavarehi, D.L. Peter, F. Sassani, Nonlinear modeling and validation of solenoid-controlled pilot-operated servovalves, IEEE/ASME Trans. Mechatron. 4 (3) (1999) 324–333.
[8] M.F. Rahman, N.C. Cheung, K.W. Lim, Position estimation in solenoid actuators, IEEE Indus. Appl. Conf. (1995) 476–484.
[9] R.R. Chladny, C.R. Koch, A.F. Lynch, Modeling automotive gas-exchange solenoid valve actuators, IEEE Trans. Magnet. 41 (3) (2005) 1155–1162.
[10] Y. Kawase, Y. Ohdachi, Dynamic analysis of automative solenoid valve using finite element method, IEEE Trans. Magnet. 27 (4) (1991) 3939–3943.

[11] C. Ifirm, Nonlinear diffusion of magnetic fields in conductive, ferromagneitc media, Int. J. Appl. Electromagnet. Mech., IOS Press, 2007. pp. 735–741.
[12] J.Y. Park, M.K. Chung, Study on hydrodynamic torque of a butterfly valve, J. Fluids Eng. 128 (2006) 190–195.
[13] T. Sarpkaya, Oblique impact of a bounded stream on a plane lamina, J. Franklin Inst. 267 (3) (1959) 229–242.
[14] T. Sarpkaya, Torque and cavitation characteristics of butterfly valves, ASME J. Appl. Mech. 28 (4) (1961) 511–518.
[15] K. Ogawa, T. Takeyoshi, Hydrodynamic characteristics of a butterfly valve-prediction of torque characteristics, ISA Trans. 34 (4) (1995) 327–333.
[16] Z. Leutwyler, C. Dalton, Resultant force, and aerodynamic torque on a symmetric disk butterfly valve in a compressible flow, J. Pressure Vessel Technol. 130 (2008).
[17] American Water Works Association, "Butterfly Valves: Torque, Head Loss, and Cavitation Analysis", First Edition, ISBN:1-58321-041-5, 2001, pp. 37.
[18] Lee, D., Nataraj, C., Mousavi, P.N., Nonlinear Model-Based Adaptive Control of a Solenoid-Valve System, in: 3rd ASME Dynamic Systems and Control Conference, Boston, Sept., 2010, pp. 13–15.